Reducing the impact of reticle CD-non-uniformity of multiple structures by dose corrections based on aerial image measurements

Ute Buttgereit*[a], Robert Birkner [a], Thomas Scheruebl [a],
Sander de Putter [b], Bernardo Kastrup [b], Jo Finders [b]
[a] Carl Zeiss SMS GmbH, Carl-Zeiss-Promenade 10, 07745 Jena, Germany;
[b]ASML, De Run 6501, 5504 DR Veldhoven, The Netherlands

ABSTRACT

For many critical lithography applications the main contributor to wafer intra-field CD variation is the reticle CD variation. Current practice is that the input data needed to correct the effect of the reticle on the wafer CD is gathered using wafer exposures and SEM or scatterometry analysis. This approach consumes valuable scanner time and adds wafer costs. In this work we evaluate the potential for Intra-Field CD non-uniformity (CDU) correction based on aerial image reticle measurements for a complex 2D structure, including peripheral structures. The application selected is a 45nm rotated brick wall structure (active area DRAM). A total of 10 line / space structures (both horizontal and vertical) through pitch represent the periphery. Mask qualification has been performed using the newly developed Zeiss WLCD32 metrology tool, which measures wafer level CD on masks using aerial imaging technology. Excellent correlation is shown between intra-field wafer data and WLCD32 data. Furthermore, a comparison is made between the correction potential of ASML DoseMapper recipes based on wafer data and on WLCD32 mask data, indicating that the potential CDU improvement via both approaches is similar. Exposures with the resulting dose recipes have been used to confirm this predicted correction potential in a realistic setting.

Keywords: aerial image measurements, reticle qualification, reticle CDU, dose correction, rotated brick wall, Intra-Field CDU, DRAM

1. BACKGROUND

1.1 Application: DRAM active area

For our demonstration we have selected a pattern representative of the active area layer of a 45nm 6F2 DRAM device [1], with a hexapole illumination condition. The pattern consists of rotated bricks that form the twincells in the final memory device. The pitch in the critical direction for this layer is 91nm (k1: 0.32). The gauges that have been used for the evaluation are CD1, CD2, CD3 and Gap. The location of these gauges is indicated in Figure 1.

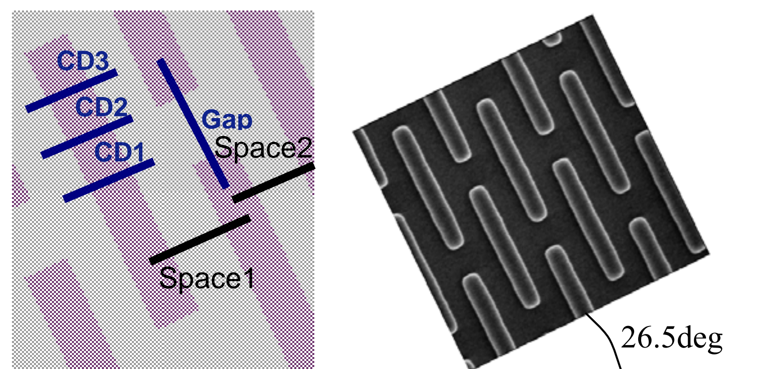

Figure 1. Left: Schematic overview of the rotated brick wall structure including the main gauges used to qualify the pattern. Right: SEM image of the structure as printed on the reticle.

CD1 represents the brick width halfway along the brick length, while CD2 and CD3 have been positioned such to divide the upper half of the brick into 3 approximately equal segments. The gap is aligned with the long axis of the brick and measures the separation between the end of one brick and the opposite end of the neighboring brick. This space must be controlled as it defines the electrical isolation between the memory cells (meaning it should be sufficiently large) but also the overlap with the contact of the actual DRAM capacitor (meaning it should be sufficiently small). The gauges CD1, CD2 and CD3 sample the brick width and represent the shape control. No dedicated OPC has been applied for this test reticle in order to print regular brick shapes, which implies that the nominal values of CD1, CD2 and CD3 are not the same. Still, the induced CD variation of these gauges with respect to their nominal values is representative of the control that would be required for a fully OPC-ed design. A DRAM periphery consists of complex structures with a minimum pitch that is approximately 1.5 – 2 times larger than the core minimum pitch. As a representation of the DRAM active area periphery five horizontal and five vertical line/space (L/S) combinations have been selected, as indicated in Table 1. The process windows of the core features and the selected L/S features have been evaluated from experimental focus exposure matrix (FEM) data acquired with SEM. The results are depicted in Figure 2. Since the isolated L/S features do not have dedicated assist features to enhance depth of focus, as would be the case for a product design, the DoF for these features is limited. Although this limitation would be relevant for an actual product design, the process windows are sufficiently large to investigate the combined CDU improvement potential for core and periphery, as is the purpose in this work.

Table 1 L/S combinations used for the representation of the periphery

Label	Orientation	CD [nm] (1X)	Pitch [nm] (1X)
P1	V	70.5	136
P2	V	80	195
P3	V	93	250
P4	V	104.5	360
P5	V	107	750
P6	H	63.5	136
P7	H	80	195
P8	H	91	250
P9	H	94	360
P10	H	95	750

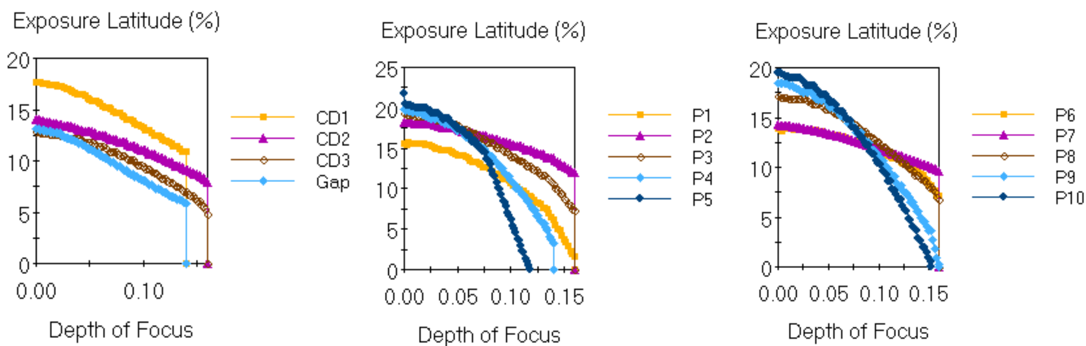

Figure 2. Left: process window evaluation (exposure latitude vs. depth of focus) for the core features. Middle: process window evaluation for the vertical L/S patterns. Right: process window evaluation for the horizontal L/S patterns. For the core line features CD variation bounds on nominal CD +/- 4.5nm have been used, while for the gap feature the nominal CD +/- 6.5nm was used. For all L/S structures the CD variation bounds have been set to nominal CD +/- 7nm.

1.2 DoseMapper

ASML's DoseMapper application allows correcting both intrawafer and intrafield CD variation profile. The corrections are determined by fitting a polynomial function of pre-defined order in x and y direction to the known CD variation of one or several features over the wafer using the sensitivity of these features CD maps to dose to determine the optimal correction procedure to minimize the variation. When using several features for the correction procedure different

weights may be applied to these features in the optimization to allow the algorithm to favor the CD control of certain critical features over the control for other less critical features. The most obvious way to obtain the relevant CD maps that serve as inputs for the fitting algorithm is to expose a product wafer and measure it with either SEM or scatterometry metrology. However, ASML also offers the so-called High-Mix approach which relies on separately providing the inputs for the intrawafer correction and the intrafield correction. In the High-Mix configuration dose maps are generated based on historical wafer measurement data and correction profiles [4]. This enables the use of dosemapper without the need to generate wafer based measurements for every layer or lot. The inputs for the intrawafer correction may for instance be taken from historical data for the same process conditions with a different exposure tool and reticle. The inputs for the intrafield CD variation can be obtained from for instance earlier exposures with the same reticle, or as is explored in this paper, from reticle metrology measurements.

1.3 Aerial image CD measurements: WLCD32

Zeiss' newly developed Wafer Level CD metrology system WLCD32 is based on proven aerial imaging technology. It measures the CD on the reticle in the wafer level plane as it is relevant to printing. By doing that it captures optical proximity effects and optical MEEF effects induced by the scanner illumination. Using the WLCD32 significantly simplifies the CD measurement especially for complex mask designs and complex 2D features [2, 3].

The WLCD32 is equipped with new Zeiss 193nm imaging and illumination optics. The LITO™-grade optics has extremely low aberrations and comes close to the quality of the scanner optics. The variable NA allows measurements up to a scanner equivalent NA of 1.4. A new 193 nm laser is used for ultra fast CD measurements of several hundred CD's per hour. The tool is equipped with two user defined aperture planes for off-axis illumination in order to illuminate the mask under the same conditions as a scanner. Additionally, newly developed "FreeForm Illumination" devices can be used to adopt the illumination not only in geometrical shape but also in intensity distribution. Furthermore, different polarizations (tangential, x, y) are available. Vector effects by high NA imaging can be taken into account by using Zeiss proprietary scanner mode.

For CD measurement the user can define several regions of interest within the field of view, which allows CD measurements on arbitrary features. The WLCD32 has CD repeatability below 0.25 nm at wafer level. Figure 3 shows the long-term CD repro measured over three days with three loads per day.

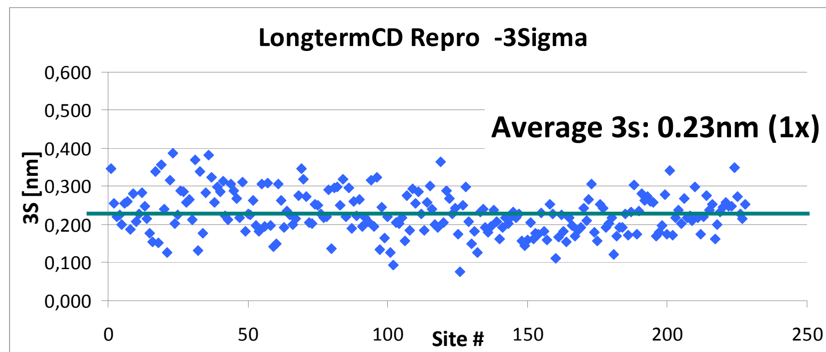

Figure 3: WLCD32 long-term CD repro measured over three days performing three loads per day. An average 3σ value of 0.23nm (wafer level) was measured.

2. MEANS AND METHODS

2.1 Exposures and wafer metrology

All exposures have been performed on TWINSCAN XT:1900i ASML immersion scanners using a hexapole diffractive optical element (DOE) as shown if Figure 4. All illumination source poles have an open angle of 20deg. The illumination settings used for the wafer exposures are: NA 1.35 (max NA), sigma (outer, inner): (0.89, 0.74), polarization: X/Y.

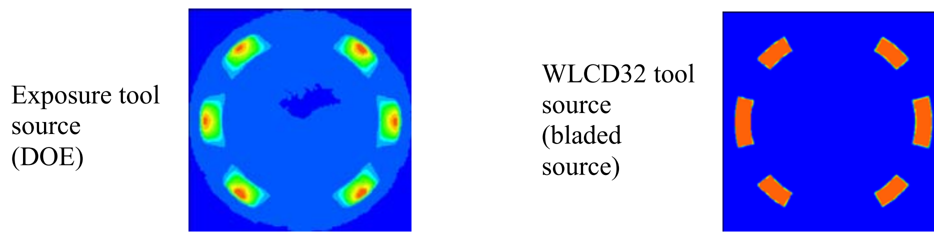

Figure 4. Left: measured illumination source on exposure tool (wafer level). Right: modeled source as used on the WLCD32 metrology tool. The exposure tool illumination source is formed with a diffractive optical element while the WLCD32 source is formed using blades, resulting in a more top-hat behavior. Furthermore, the exposure tool source has a design pole angle of 20deg for all poles, whereas the exposure source used for WLCD32 measurement has a design open angle of 30deg for the two poles incident with the horizontal center axis.

The nominal exposure dose was taken such that CD1 prints at 40nm after wafer development. The schematic reticle layout is shown in Figure 5. The rotated BW structures are placed on a 12x7 module grid. The L/S patterns used to represent the periphery are placed on a 6x6 grid, in between the core pattern modules. SEM measurements have been acquired for 30 full fields on the wafer. The Intra-Field data has been acquired by averaging CD measurements on corresponding modules for the 30 different sampled fields.

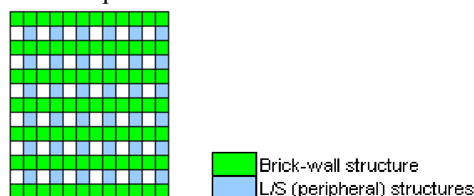

Figure 5. Reticle module layout indicating the relative positions of the core patterns and the L/S patterns used to represent the periphery of the device

The process stack used for the wafer exposures consists of 105 nm ARC29SR (Brewer Science), 95 nm TArFP6i001 (TOK), and 90 nm TCX041 (JSR). A post-exposure bake step has been applied before the development. SEM measurements have been performed directly on the resist pattern (no etch step applied). These measurements have been performed with a Hitachi CG4000 (magnification 100, threshold 75, Voltage 500).
Two sets of wafer data have been generated. The first wafer data set, labeled “set 1” throughout the text, has been acquired in May 2009 on an ASML XT:1900i tool within ASML’s own clean room facilities (Veldhoven, The Netherlands). This data set has been used to generate and evaluate the several dose recipes used for correction. The second wafer data set, labeled “set 2” throughout the text, has been acquired at IMEC facilities (Leuven, Belgium) on a different ASML XT:1900i tool in December 2009. This second data set has been acquired to verify that the predicted corrections can indeed be achieved in a different setting.

2.2 Reticle metrology

The CD uniformity of the reticle was measured by WLCD32. The following illumination conditions have been applied: NA 1.35, sigma (outer, inner): (0.89, 0.74), polarization: X/Y. An available sigma aperture was used which comes close to the shape of the illumination source of the scanner. The applied aperture is a hexapole aperture with an opening angle of 20°, respectively 30° for the poles sitting on the x-axis. The CD uniformity was measured for the rotated BW having a 91nm pitch. A grid of 12x 7 positions was measured over the reticle.
The WLCD32 captures the aerial image of the rotated BW structures. For CD evaluation the WLCD SW allows to place a Region of Interest (ROI) over each single feature or to place a ROI over an array of features of interest (Figure 6), analyzing the desired CD values of the features in this array. The ROI can be placed in arbitrary directions, meaning that angles can be considered which is important for tilted structures. As can be seen in Figure 6 the CDx, which corresponds to CD1 in our case, and CDy with respect to the ROI orientation can be analyzed automatically in the ROI array. The CDx and CDy for each feature are measured in the centre of gravity of the feature which is determined with sub-pixel resolution. The threshold is set in the way that the average CD is 40nm for CD1.

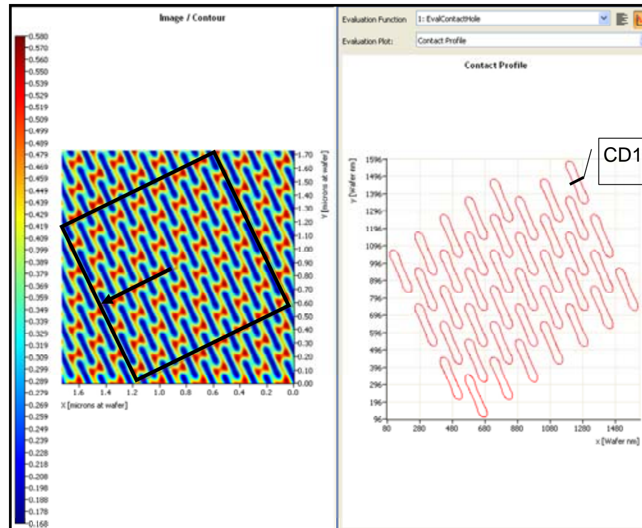

Figure 6: Left: WLCD32 CD analysis showing the aerial image of the tilted BW structures and the ROI covering an array of features. Right: CD profile lines of the BW structure for a threshold leading to an average CD of 40nm for CD1

Additionally to the CD analysis a contour plot according to a desired threshold can be extracted, which is shown in Figure 7. For the CD measurement in the current case a more complex CD analysis was required measuring the line CD1, CD2, CD3, the space CD space1 and space2 and the gap. The leading CD to define the threshold is CD1 with a target CD of 40nm.

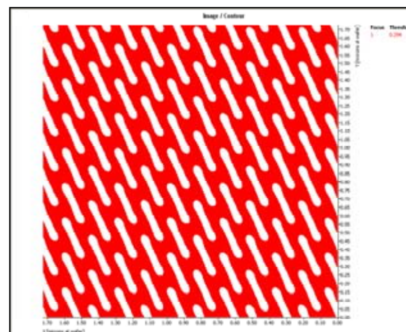

Figure 7: WLCD32 contour plot for the BW structure at the threshold leading to 40nm CD1.

2.3 Off-line aerial image analysis

For the more complex analysis of the WLCD32 aerial images a dedicated off-line routine has been employed. To analyze the images for the different reticle locations the intensity images have first been thresholded with an arbitrary threshold value to get closed isophotes in the intensity image representing the brick contours. Next the centers of gravity of the resulting contours have been used as a reproducible reference grid to define the gauges, as indicated in Figure 8. The CD measurements on the gauges have been obtained by sampling intensity profiles along the gauges with bicubic interpolation with a high sub-pixel resolution and then detecting the points where the intensity is closest to a preset threshold. For each image a fixed exclusion boundary has been used to prevent sampling incomplete bricks. Since the positioning of the bricks within the field of view is not the same for each image, the number of samples obtained in this manner varies for each image. To obtain a consistent strategy the number of samples used for each image has been limited to the minimum number of bricks within any field of view. This led to a total averaging of 54 bricks for each position. The threshold has been determined by repeatedly applying this procedure to determine the threshold value giving a resultant value for CD1 of 40nm.

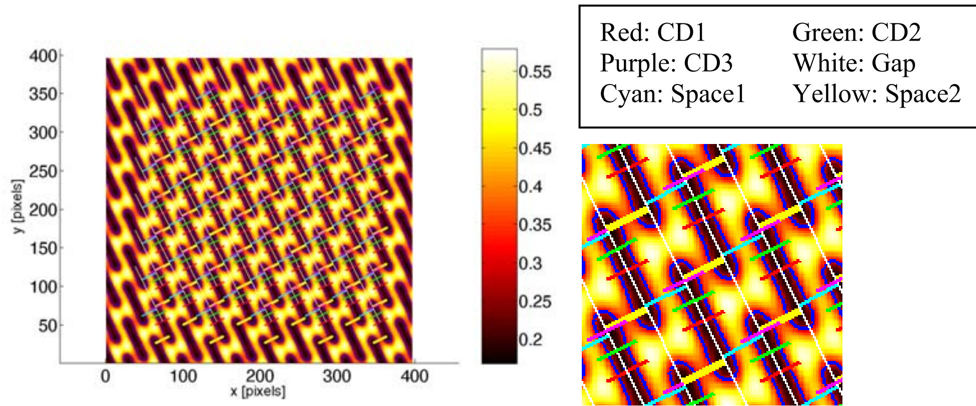

Figure 8 Analysis of aerial images for each reticle position. The blue contour depicts the intensity isophote contour for the threshold resulting in an average CD value of 40nm for the CD1 gauge.

2.4 Dose correction recipes

Dose correction recipes have been created using the ASML DoseMapper application. For the wafer based recipe the Intra-Field CD data for the brickwall line gauges (CD1, CD2, CD3 and gap) has been used as input data, all with equal weights. For the DoseMapper recipes based on the WLCD32 data a correlation analysis between the intrafield wafer data and the WLCD32 data has been performed. The regression coefficients between the aerial image data and the wafer data were found to be unequal to 1 (see also Table 4 and Figure 11). This is partly caused by the fact that the aerial image MEEF is expected to be smaller than the full resist MEEF, due to contrast loss effects induced by the resist, and possibly also partly by the difference in the illumination sources between the two experiments. In order to generate meaningful dose correction recipes based on the WLCD32 data the CD variation has been scaled around its nominal value with the individual regression coefficients deduced for the different gauges (see also section 3.2). The resulting scaled data for the line gauges has been directly used as the input for the dose correction recipe generation, again using equal weights for each gauge. Dose sensitivities for each gauge, both core and periphery, have been obtained by fitting dose sensitivities on wafer FEM data. For the comparison, several different correction strategies have been applied. These are listed in Table 2. For recipes A3 and B3 the known CD variation for the core features has been combined with a flat CD response (all CD values equal to nominal) for all periphery features in the input CD data. This approach may be useful in the case that the actual intrafield CD data for these features are not available (for instance to reduce the cost of reticle metrology) but there still is a need for control on these features. The effect of the approach is that the deviation of the intrafield CD variation with respect to the nominal (unknown) fingerprint is being limited, to avoid introducing unnecessarily large deviations for these structures. For all recipes the weights of the core features have been taken equal: 1.0. For recipe A3 and B3, the periphery features have been taken into account in the optimization with a reduced weight: 0.25 for all 10 features.

Table 2 Correction recipes details

	Input source	**Input gauges**	**Polynomial order slit**	**Polynomial order scan**
Recipe A1	Wafer data set 1	Core	6	4
Recipe A2	WLCD32	Core	6	4
Recipe A3	WLCD32	Core + flat CD profile periphery	6	4
Recipe B1	Wafer data set 1	Core	6	6
Recipe B2	WLCD32	Core	6	6
Recipe B3	WLCD32	Core + flat CD profile periphery	6	6

3. RESULTS

3.1 WLCD32 analysis results

Figure 9 shows the intrafield CD values obtained for the different gauges from the WLCD32 data. The line gauges (CD1, CD2, and CD3) all show the same distinct fingerprint. There is a relatively large CD deviation for the uppermost scan row on the reticle. The fingerprint for the space gauges (Space1, Space2 and gap) is also similar and opposite to the line gauges fingerprints, indicating that the CD variation on the reticle is largely correlated for the different gauges. This observation has been quantified in Table 3. The correlations between the several gauges are very high, indicating that the reticle writing errors in all directions are coupled, indicating a global bias like variation. This effect is also illustrated in Figure 10, which shows the fingerprints for the main brick width and the isolation gap, both for the WLCD32 data and the wafer average field data. The CD maps for space1 and space2 have been gathered mainly for verification and are shown for completeness. Since the space gauges are coupled to the line gauges via the constant pitch, these measurements do not add essential information for the correction strategy. Therefore these gauges have not been included in the analysis.

Table 3 WLCD32 analysis results overview

		Correlation coefficients		
	CDU (3σ) [nm]	**CD1**	**CD2**	**CD3**
CD1	2.0			
CD2	2.6	0.99		
CD3	3.4	0.99	0.99	
Gap	5.0	-0.95	-0.95	-0.96

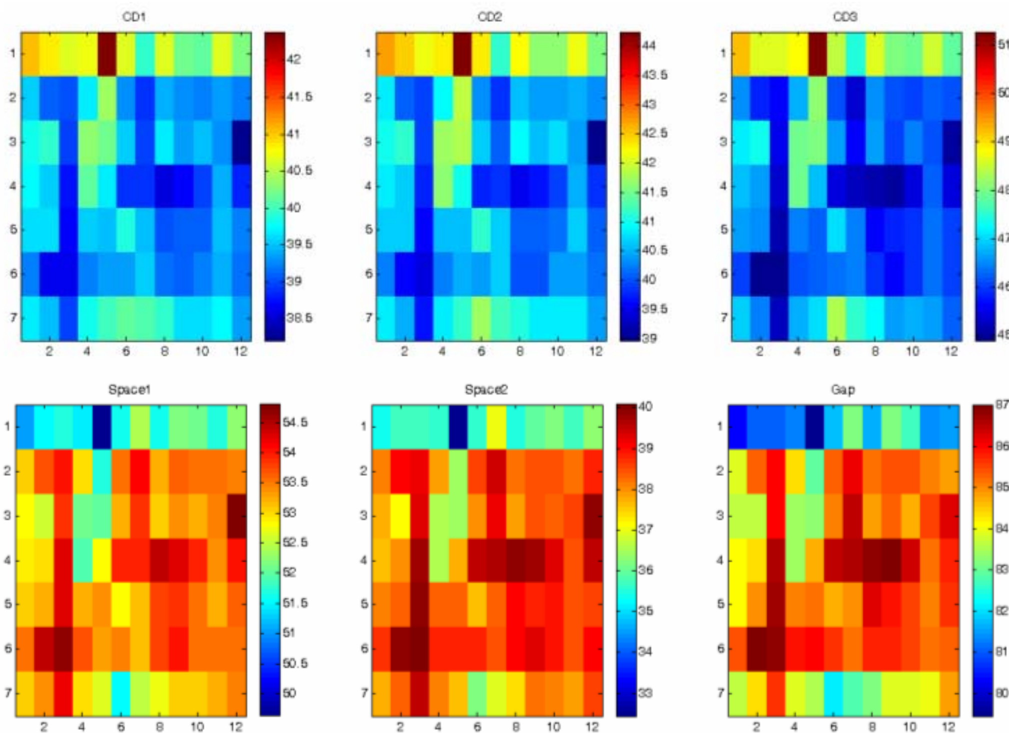

Figure 9: Intrafield CDU data [nm] from the WLCD32 measurements analysis.

3.2 Correlation analysis WLCD32 and uncorrected wafer results

Table 4, Figure 10, and Figure 11 show the correlation between the wafer intrafield data and the WLCD32 analysis results for the four gauges on the core. The CDU for the wafer data is consistently higher than the CDU for the WLCD32 analysis results, as was expected. This is also evident from the regression coefficients between wafer data set 1 and the WLCD32 data. The correlation between the WLCD32 data and the data from set 1 is high, indicating that the wafer intrafield

fingerprint is dominated by the reticle effect. This is also reflected in the limited CDU variation between wafer data set 1 and wafer data set 2. The impact of the difference in facilities and exposure tool on the CDU is limited relative to the contribution of the reticle, which is the constant factor between these two exposures.

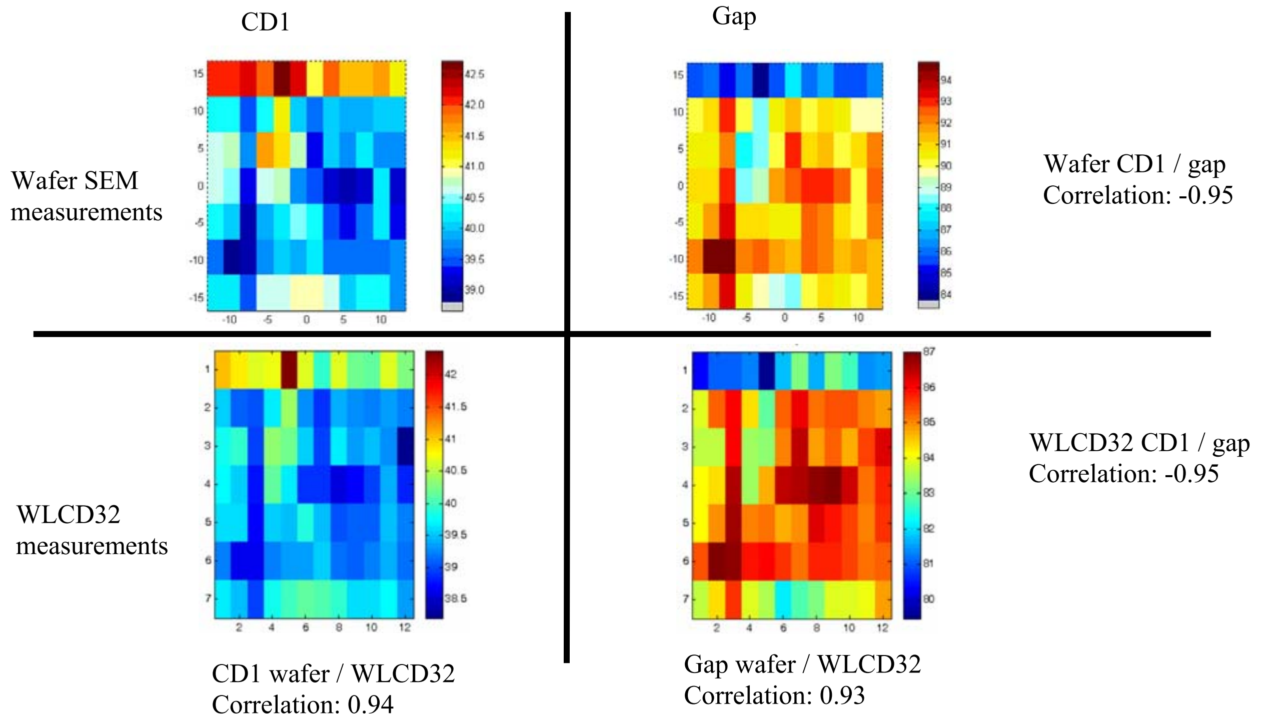

Figure 10 Average field CD maps for the principal brick width and the isolation gap feature for wafer data set 1 and the WLCD32 based CD data.

Table 4 Correlation analysis wafer data

	CDU (3σ) [nm] WLCD32 data	CDU (3σ) [nm] wafer data set 1	CDU (3σ) [nm] wafer data set 2	Correlation coefficient WLCD32 / wafer data set 1	Regression coefficient wafer data set 1 / WLCD32 data
CD1	2.0	2.6	2.7	0.94	1.23
CD2	2.6	3.3	3.6	0.88	1.12
CD3	3.4	4.8	4.3	0.95	1.33
Gap	5.0	6.9	6.4	0.93	1.29

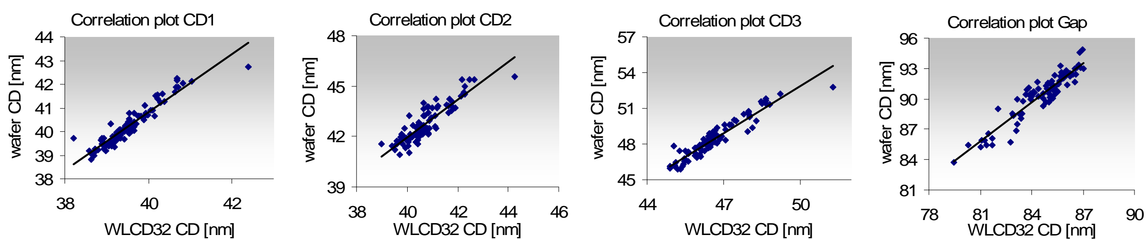

Figure 11: Correlation plots of WLCD32 CD data versus wafer CD data. See Table 4 for the corresponding correlation coefficients and regression coefficients.

3.3 DoseMapper corrections – predictions and wafer results

All wafer data in this section has been obtained from exposure set 2. Figure 12 shows wafer CD maps for the core features CD1 and gap both without dose correction and with dose corrections. The CD fingerprint clearly has been reduced after the dose corrections.

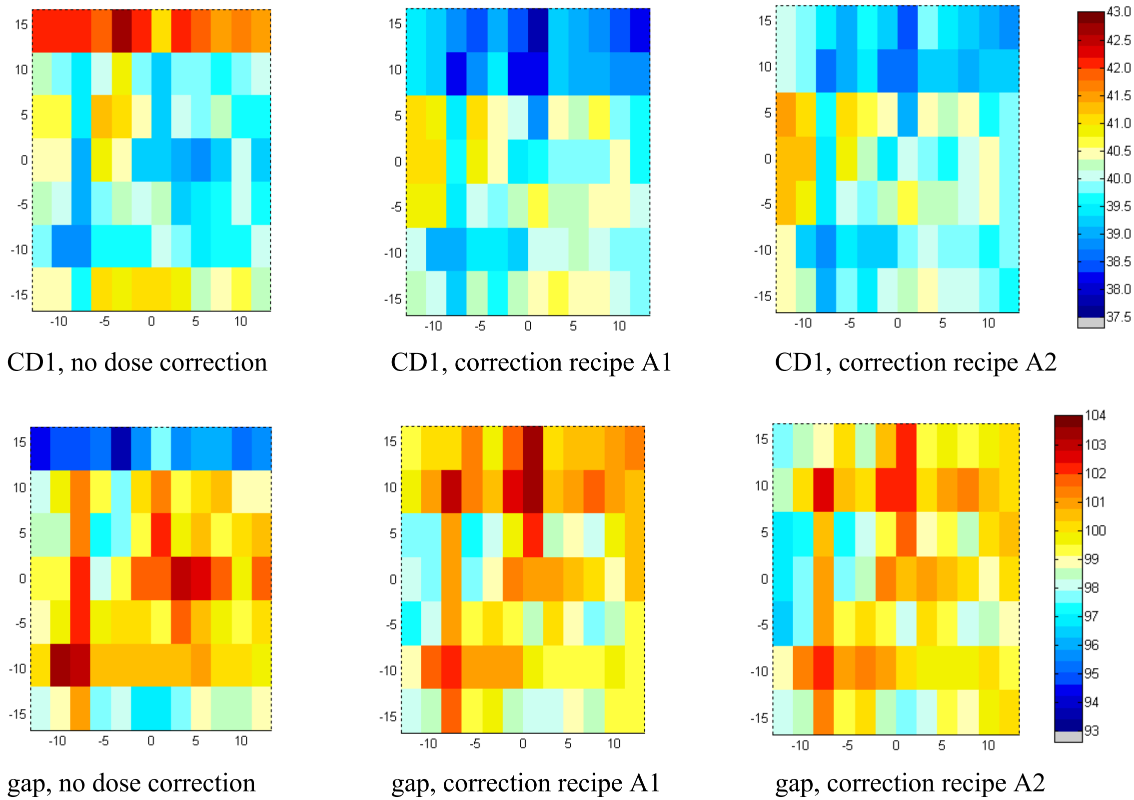

Figure 12 CD fingerprints for core features CD1 and gap without dose correction (left), with correction recipe A1 (wafer data based correction, middle column) and recipe A2 (WLCD32 data based recipe, right column)

Figure 13 shows a comparison between the uncorrected intrafield CDU, the predicted intrafield CDU and the measured intrafield CDU for both a wafer based correction recipe (A1) and a WLCD32 based correction recipe (A2). The DoseMapper predictions indicate that a significant improvement of CDU can be achieved for the core features, at the cost of deteriorated CDU numbers for the peripheral features. The predicted CDU numbers are very similar for the wafer based recipes and the WLCD32 based recipe. The same holds for the actual measured intrafield CDU data. There is a good match between the predicted CDU after correction and the measured CD after correction. The largest deviation between predictions and measurements are seen for the peripheral features.

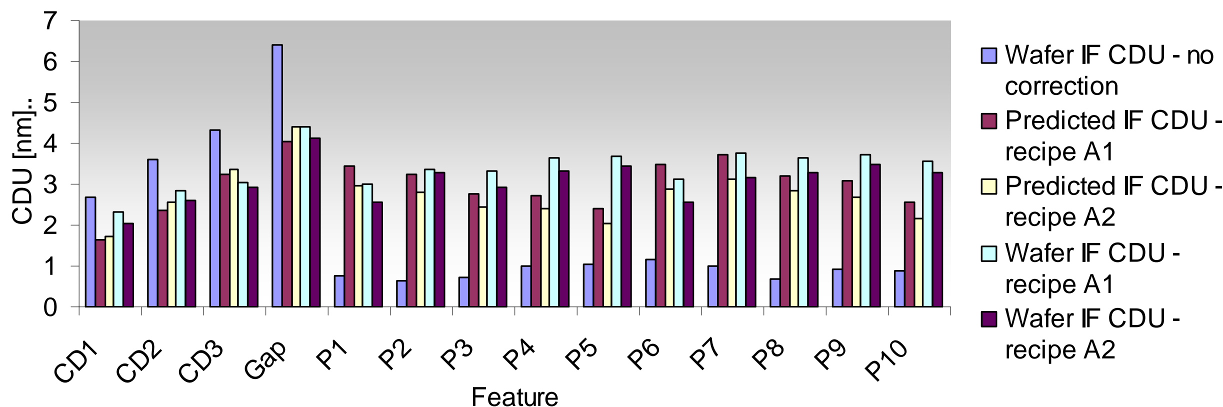

Figure 13 Analysis results wafer data set 2. Comparison of the uncorrected intrafield CDU with the predicted and measured CDU after correction with a wafer data based recipe (A1) and a WLCD32 data based recipe (A2). Polynomial order slit profile: 6. Polynomial order scan profile: 4.

Figure 14 shows the experimental results for both the wafer based correction recipes (A1, B1) and the WLCD32 based correction recipes (A2, B2), both for a 4-th order scan profile (A1, A2) and a 6-th order scan profile (B1, B2). Using a higher polynomial order for the scan profile clearly helps to reduce the CDU, particularly for the periphery. This statement holds both for the WLCD32 based correction recipe and the wafer data based reticle. The overall gain however, is limited.

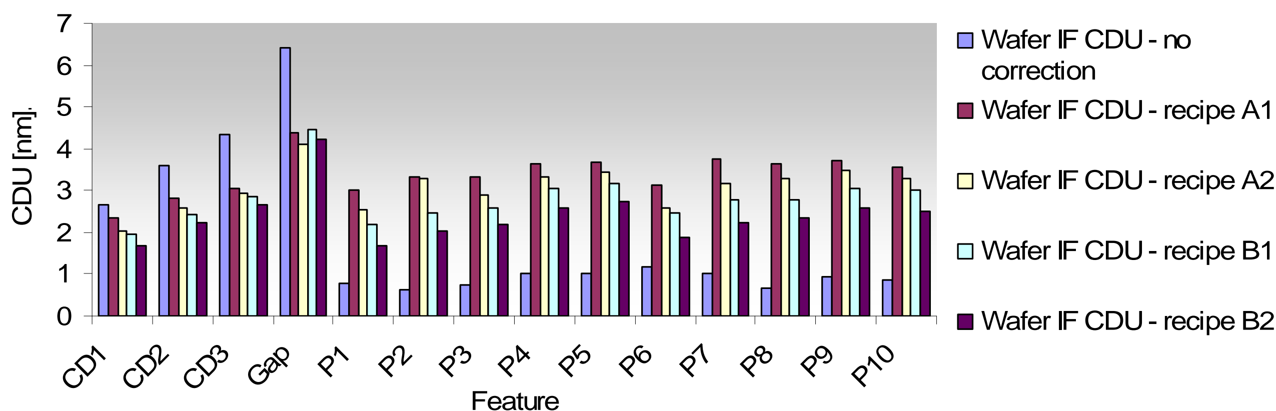

Figure 14 Analysis results wafer data set 2. Comparison of the uncorrected intrafield CDU with the measured CDU based on correction with a wafer data based recipe (A1, B1) and a WLCD32 data based recipe (A2, B2). A1, A2: polynomial order slit profile: 6, polynomial order scan profile: 4. B1, B2: polynomial order slit profile: 6, polynomial order scan profile: 6.

Figure 15 shows a comparison between the uncorrected intrafield CDU data and the CDU after correction with WLCD32 recipe based on only the core gauges (A2) and a recipe which takes into account a flat CD input for the peripheral features (A3). The DoseMapper prediction indicates that a significant gain may be achieved for the periphery CDU without having to sacrifice CDU performance for the core gauges. Although the experimental intrafield CDU data for the peripheral features is again slightly higher than the predicted performance, the positive effect of taking into account the sensitivities for the peripheral features is clearly visible in the experimental data as well.

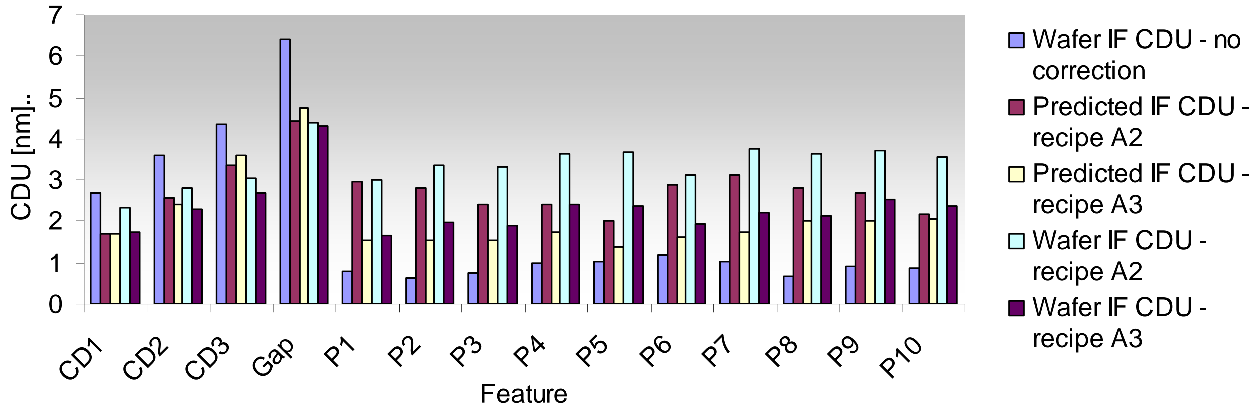

Figure 15 Analysis results wafer data set 2. Comparison of the uncorrected intrafield CDU with the measured CDU based on correction with WLCD32 data based recipes based on only the core gauges (A2) and a recipe taking into account a flat CD response for the peripheral features as well (A3). Polynomial order slit profile: 6. Polynomial order scan profile: 4.

4. DISCUSSION

In this work we have evaluated the potential of using WLCD32 reticle measurement data to generate the dose correction recipe for ASML's DoseMapper application for intrafield wafer CDU correction (HighMix configuration) for 45nm critical DRAM layer. These first results are very encouraging. Still, there are some procedural steps used in this study that would differ from a production implementation of the proposed method. First of all we have used the intra-field wafer data to determine the regression coefficients needed to determine the scaling factor for the WLCD32 intrafield maps before generating the dose correction recipes. In the intended flow, the wafer data will not be available for the specific reticle for which the WLCD32 measurements have been taken. This means that the scaling factors will need to be derived either from historical data from a previous reticle (which implies that the approach cannot be followed for the first reticle for a layer) or must be predicted using simulation tools. Although this limitation may slightly affect the quality for the corrections in a more realistic setting it does not interfere with the purpose of this study which was to show the suitability of the proposed approach. Secondly, the reticle used in this study has a very distinct fingerprint. There is a strong CD deviation on the upper row of the reticle only. The correction potential for the intra-field wafer CDU strongly depends on the quality of the reticle for the layer. Also, the locations of the peripheral features on this reticle are separated from the locations of the core structures. This may have an effect on the interaction between the CDU performance of the core gauges versus the peripheral gauges. For a production reticle this layout may be different and this may have an effect on the applicability of this approach for different applications.

However, the reticle used in this study was not specifically designed for this study and there is no reason to assume that reticle CD variations as encountered in this study will not occur more often. In fact, the approach that is proposed in this paper may help to achieve acceptable yield for reticles that would otherwise need to be rejected, thus reducing the impact of reticle costs.

The weights used for the periphery for correction recipes A3 and B3 are empirical. We did not yet derive a strategy that will allow determining the optimal weights for every (sub)critical reticle feature for which the reticle fingerprint is unknown. Without such a strategy the approach is still useful however. In any situation meaningful weights can be iteratively determined by finding the balance between the weights for the critical and less critical features that does not result in significant deterioration of the critical features CDU with respect to the optimum correction for these critical features. This way, some level of control can be added for all less critical features without having to sacrifice any performance for the critical features themselves. One possible implementation is to measure the reticle fingerprint for the most critical features only and simulate the sensitivities for the critical features combined with a large set of gauges distributed over the design GDS using a calibrated large field simulator/scanner tuner such as LithoTuner (Brion, ASML). In this manner it can be assured that the optimal CDU is achieved for the critical features while minimizing the risk of introducing unwanted CD variation elsewhere in the design.

5. CONCLUSIONS

We have shown the potential of using WLCD32 reticle metrology data to improve intrafield CDU performance for a critical layer for a 45nm DRAM device. The results show that the corrections that are achievable via the WLCD32 reticle data are as good as the intrafield corrections that may be achieved based on direct wafer data for the same reticle from a different exposure tool. This approach enables performing reticle specific dose corrections, that are independent of the specific exposure tool, without consuming valuable scanner time. We have proven high accuracy for the WLCD32 aerial image metrology application by showing excellent correlation with wafer data. Finally we have shown that knowledge of peripheral structures sensitivities can be employed to improve the overall combined CDU numbers, without having to incorporate actual measurement data of these features.

ACKNOWLEDGEMENTS

The authors would like to thank Mariette Berende–Hogendijk, Yin Fong Choi, Eddy van der Heijden, Dorothe Oorschot, Kees Ricken, Charles Schaap, Nicole Schoumans, and Amir Sharomi of ASML for their contributions in securing the wafer data. Furthermore we owe gratitude to IMEC, Leuven, Belgium for allowing us to perform exposures in their facilities.

REFERENCES

1. Changhyun Cho, Sangho Song, Sangho Kim, Sungho Jang, Sungsam Lee, Hyungtak Kim, Yangsoo Sung, Sangmin Jeon, Gisung Yeo, Youngsun Kim, Yungi Kim, Gyoyoung Jin and Kinam Kim, A 6F2 DRAM Technology in 60nm era for Gigabit Densities, 2005 Symposium on VLSI Technology Digest of Technical Papers (2005) pp36-37.
2. Sven Martin, Holger Seitz, Wolfgang Degel, Ute Buttgereit, Thomas Scherübl, "WLCD: A new System for Wafer Level CD Metrology on Photomasks", Proc. SPIE, Volume 7272 (2009), pp. 72722T-72722T-9 (2009).
3. F.Dufaye, S.Gough, F.Sundermann, V.Farysa,H.Miyashita, L.Sartelli, F. Perissinotti, U.Buttgereit, S.Perlitz, R.Birkner, "Mask phase and transmission variation effects on wafer critical dimensions for nodes 65nm and 45nm", EMLC (2010).
4. K. Nafus, T. Shimoaoki, M. Enomoto, H. Shite, T. Otsuka, H. Kosugi, T. Shibata, J. Mallmann, R. Maas, C. Verspaget, E. van der Heijden, E. van Setten, J. Finders, S. Wang, N. Boudou, C. Zoldesi, Improvements in process performance for immersion technology high volume manufacturing. Proceedings of the SPIE, Volume 7273 (2009)., pp. 727338-727338-11 (2009).